

Supporting Information

**A Novel Long-alkyl Chains Acylhydrazone-based Supramolecular
Polymer Material for Ultrasensitive Detection and Separation of
Multianalytes**

Zhi-Yuan Yin, Jing Han Hu*, Qing-Qing Fu, Kai Gui and Ying Yao

College of Chemical and Biological Engineering, Lanzhou Jiaotong University, Lanzhou,
gansu, 730070, P. R. China

Table of contents

Materials and methods

Experimental Section

Scheme 1 The synthesis of G.

Fig. S1 ^1H NMR spectra of G.

Fig. S2 ^{13}C NMR spectra of G.

Fig. S3 HRMS spectra of G.

Table S1. Gelation properties of gelator G.

Fig. S4 Fluorescence spectra of OGV (1.0%, in DMSO) in the presence of various anions (Ca^{2+} , Mg^{2+} , Pb^{2+} , Ni^{2+} , Co^{2+} , Hg^{2+} , Zn^{2+} , Cd^{2+} , Ag^+ , Cr^{3+} , Cu^{2+} , Al^{3+} , Fe^{3+} , Ba^{2+} , La^{3+} , Eu^{3+} and Tb^{3+} , respectively, using their 0.1 mol L^{-1} sodium or potassium salts water solution as the sources) at room temperature ($\lambda_{\text{ex}}=310$ nm).

Table S2. Calculation the detection line of HgG, FeG, HgG + CN^- and FeG + H_2PO_4^- .

Fig. S5 Fluorescent titrations spectra of HgG and FeG and linear fitting of titration curves of HgG and FeG.

Table S2 Calculation the detection line of HgG, FeG, HgG + CN^- and FeG + H_2PO_4^- .

Fig. S6 Fluorescent titrations spectra of (a) HgG and (c) FeG and linear fitting of titration curves for (b) HgG and (d) FeG.

Fig. S7 Fluorescence spectra of HgG (1.0%, in DMSO) in the presence of various anions (F^- , Cl^- , Br^- , I^- , AcO^- , H_2PO_4^- , HSO_4^- , N_3^- , SCN^- , S_2^- , ClO_4^- , and CN^-), respectively, using their 0.1 mol L^{-1} sodium or potassium salts water solution as the sources) at room temperature ($\lambda_{\text{ex}}=310$ nm).

Fig. S8 Fluorescence spectra of FeG (1.0%, in DMSO) in the presence of various anions (F^- , Cl^- , Br^- , I^- , AcO^- , H_2PO_4^- , HSO_4^- , N_3^- , SCN^- , S_2^- , ClO_4^- , and CN^-), respectively, using their 0.1 mol L^{-1} sodium or potassium salts water solution as the sources, at room temperature ($\lambda_{\text{ex}}=310$ nm).

Fig. S9 The linear fitting of titration curves for (a) HgG+ CN^- and (b) FeG+ H_2PO_4^- .

Fig. S10 FT-IR spectra of (a) powder G and xerogel of organogel OGV (b) xerogel of OGV, HgG and HgG treated with CN^- , (c) xerogel of OGV, FeG and FeG treated with H_2PO_4^- .

Fig. S11 Powder XRD pattern of (a) organogel OGV and metallogel (HgG and FeG), (b) organogel OGV, HgG and HgG treated with CN^- , (c) organogel OGV, FeG and FeG treated with H_2PO_4^- .

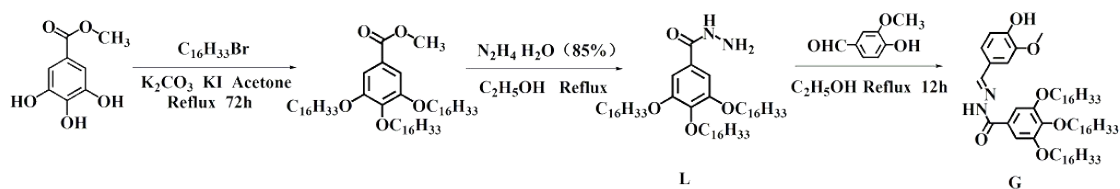
Fig. S12 SEM image of (a) HgG xerogel; (b) FeG xerogel ; (c) HgG xerogel treated with CN^- ; (d) FeG xerogel treated with H_2PO_4^- .

Materials and physical methods

All reagents and starting materials were obtained from commercial suppliers and used as received unless otherwise noted. All anions were used as sodium or potassium salts while all cations were used as the perchlorate salts, which were purchased from Alfa Aesar and used as received. Fresh double distilled water was used throughout the experiment. Nuclear magnetic resonance (NMR) spectra were recorded on Varian Mercury 400 and Varian Inova 600 instruments. Mass spectra were recorded on a Bruker Esquire 6000 MS instrument. The X-ray Diffraction analysis (XRD) was performed in a transmission mode with a Rigaku RINT2000 diffractometer equipped with graphite monochromated CuK α radiation ($\lambda=1.54073$ Å). The morphologies and Sizes of the xerogels were characterized using field emission scanning electron microscopy (FE-SEM, JSM-6701F) at an accelerating voltage of 8kV. The infrared spectra were performed on a Digilab FTS-3000 Fourier transform-infrared spectrophotometer. Melting points were measured on an X-4 digital melting-point apparatus (uncorrected). Fluorescence spectra were recorded on a Shimadzu RF-5301PC spectrofluorophotometer.

Experimental Section

As shown in **Scheme 1**, the compound 3, 4, 5-tris (hexadecyloxy) benzohydrazide was synthesized according to the literature-reported methods.²¹ The G was synthesized as follow: vanilline (1mmol), 3,4,5-tris(hexadecyloxy)-benzohydrazide (1 m mol) and acetic acid (0.1 m L, as a catalyst) were added to ethanol (20 m L). Then the reaction mixture was stirred at 80°C for 24 h, after the solvent was removed, the precipitated G was yielded and recrystallized with CHCl₃–CH₂CH₃OH to get the pour solid G. (Yield: 80%). m.p.126-128°C. ¹H NMR (500 MHz, CDCl₃) δ 9.12, 8.18, 7.53, 7.26, 7.01, 6.92, 5.91, 4.01, 3.96, 1.80, 1.58, 1.46, 1.26, 0.88. (**Fig S1**). ¹³C NMR (126 MHz, CDCl₃) δ 185.03, 153.25, 148.36, 147.14, 141.56, 130.89, 126.14, 114.03, 107.69, 105.90, 76.77, 73.57, 69.39, 56.21, 31.94, 30.93, 29.74, 29.38, 26.12, 22.70, 14.12. (**Fig S2**). ESI-MS m/z: calcd for C₁₆H₁₁₀N₂O₆ [G+ H]⁺: 991.84; found: 991.84(**Fig S3**).



Scheme 1 The synthesis of G.

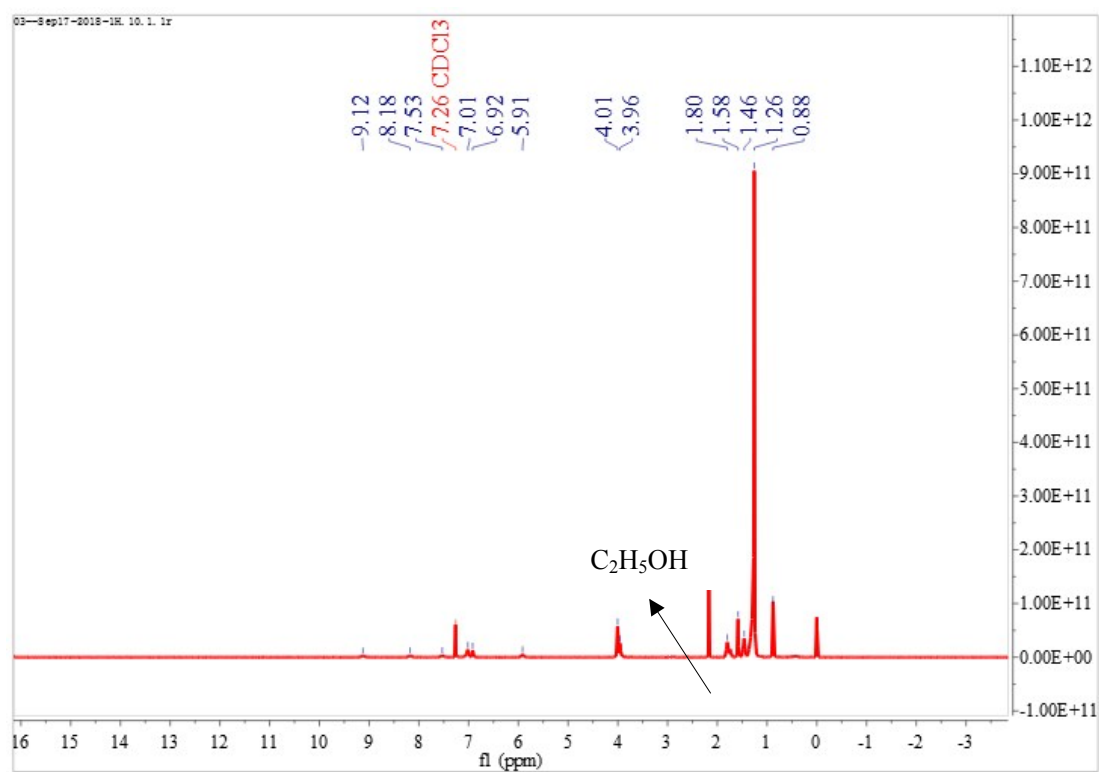


Fig. S1 ¹H NMR spectra of G.

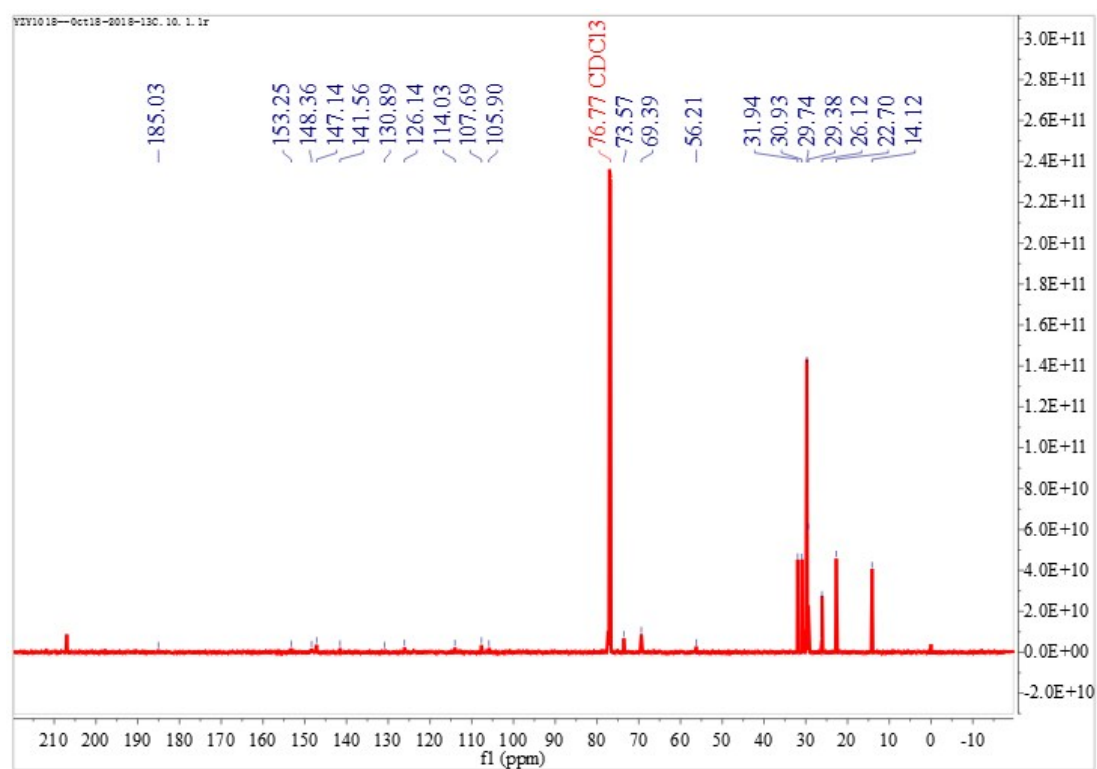


Fig. S2 ¹³C NMR spectra of G.

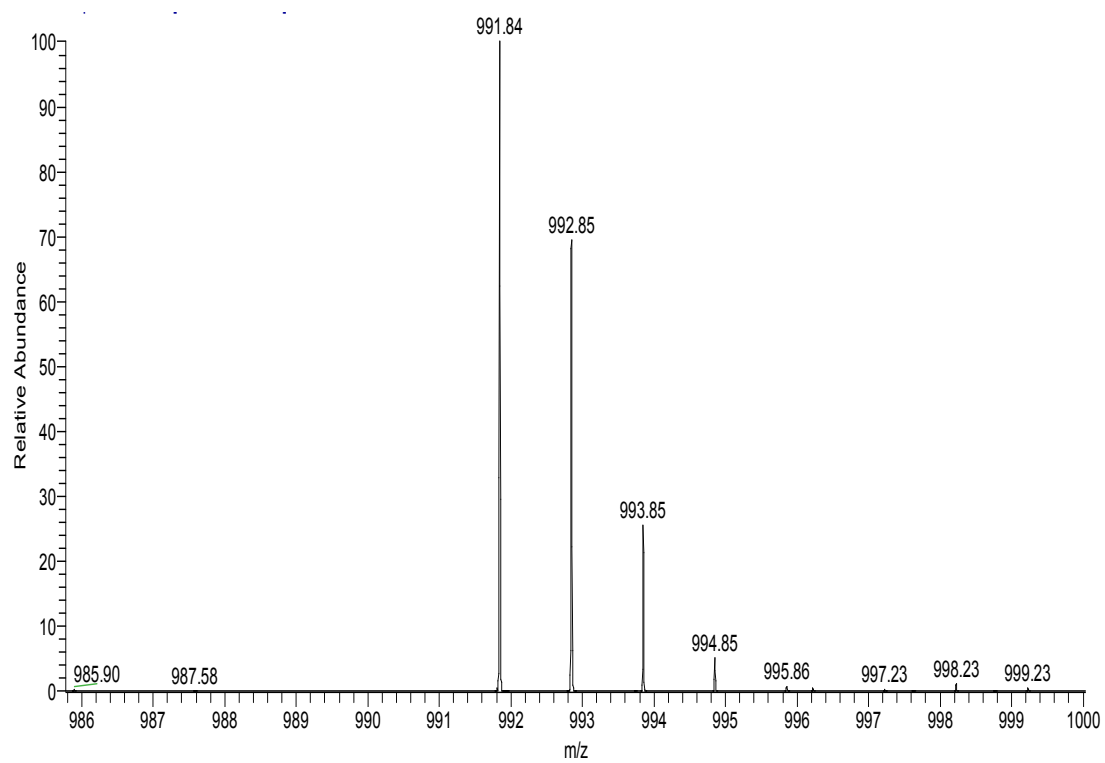


Fig. S3 MAS spectra of G.

Solvent	Gelation Behavior ^a	Gelating time	MGC ^b	MGT ^c
MeOH	G	3min	1	49
MeOH-H ₂ O	SP	—	—	—
EtOH	SP	—	—	—
EtOH-H ₂ O	SP	—	—	—
i-PrOH	SP	—	—	—
n-BuOH	SP	—	—	—
Acetone	SP	—	—	—
Acetonitrile	SP	—	—	—
DMSO	G	1min	1	53
DMSO-H ₂ O	SP	—	—	—
DMF	SP	—	—	—
DMF-H ₂ O	SP	—	—	—
THF	S	—	—	—
Toluene	S	—	—	—
Chloroform	S	—	—	—
Methylene chloride	S	—	—	—
Carbon tetrachloride	S	—	—	—

^aG, gel; S, solution; SP, solution precipitate.

^bMGC is the minimum gelator concentration (w/v%, 10 mg mL⁻¹ = 1%).

^cMGT is the gelation temperature (°C) at the minimum gelator concentration

Table S1. Gelation properties of gelator G.

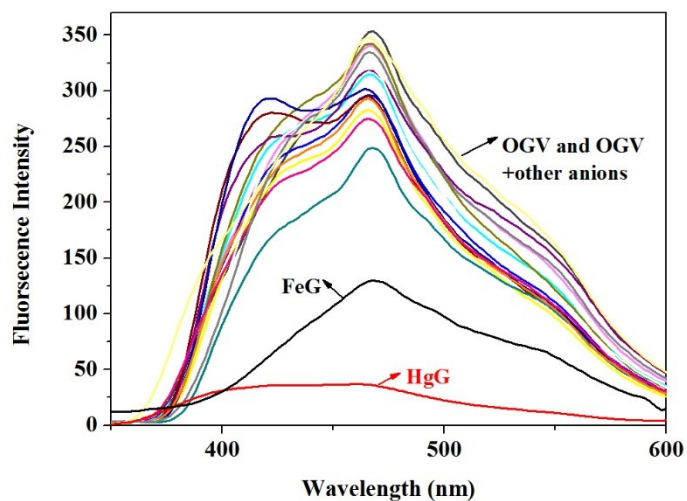


Fig. S4 Fluorescence spectra of OGV (1.0%, in DMSO) in the presence of various anions (Ca^{2+} , Mg^{2+} , Pb^{2+} , Ni^{2+} , Co^{2+} , Hg^{2+} , Zn^{2+} , Cd^{2+} , Ag^{+} , Cr^{3+} , Cu^{2+} , Al^{3+} , Fe^{3+} , Ba^{2+} , La^{3+} , Eu^{3+} and Tb^{3+} , respectively, using their 0.1 mol L^{-1} sodium or potassium salts water solution as the sources) at room temperature ($\lambda_{\text{ex}} = 310 \text{ nm}$).

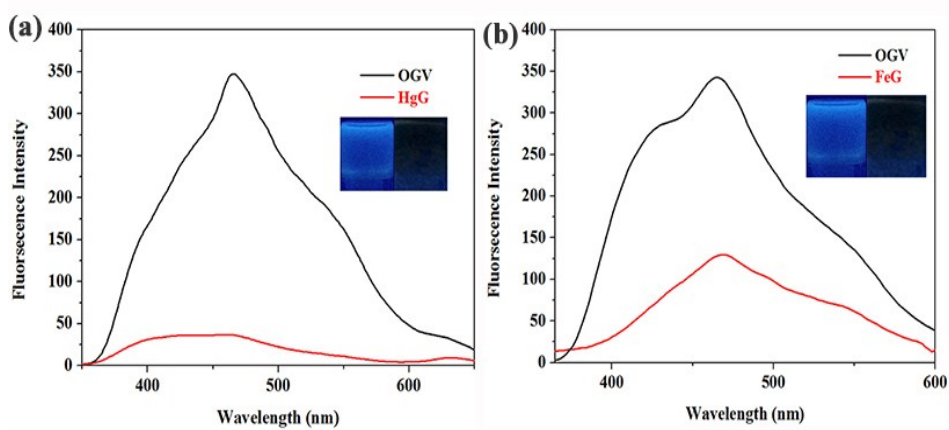


Fig. S5 Fluorescence spectra of OGV (1.0%, in DMSO) and OGV in the presence of Hg^{2+} and Fe^{3+} at room temperature ($\lambda_{\text{ex}} = 310 \text{ nm}$).

	δ	A	S	LOD
HgG	1.49	-1417.2939	-1383.84236 $\times 10^6$	3.15 $\times 10^{-9}$
FeG		-525.3651	-613.16189 $\times 10^6$	2.83 $\times 10^{-9}$
HgG + CN^-		400.4766	480.88306 $\times 10^6$	3.72 $\times 10^{-9}$
Fe G + H_2PO_4^-		633.611	633.01123 $\times 10^6$	2.35 $\times 10^{-9}$

Calculation formula of LOD

Linear Equation: $y = Ax + B$

$$\text{LOD} = K \times \frac{\delta}{S} (K = 3)$$

$$\delta = \sqrt{\frac{\sum (F_i - F_0)^2}{N-1}} (N = 20)$$

$$S = A \times 10^6$$

State, F_i : the fluorescence intensity of OGV at $\lambda_{\text{ex}} = 310$ nm; F_0 : the average of 20 times fluorescence intensity of OGV at $\lambda_{\text{ex}} = 310$ nm; **A**: slope of linear fitting of fluorescence titration;

B: intercept of linear fitting of fluorescence titration.

Table S2 Calculation the detection line of HgG, FeG, HgG + CN^- and FeG + H_2PO_4^- .

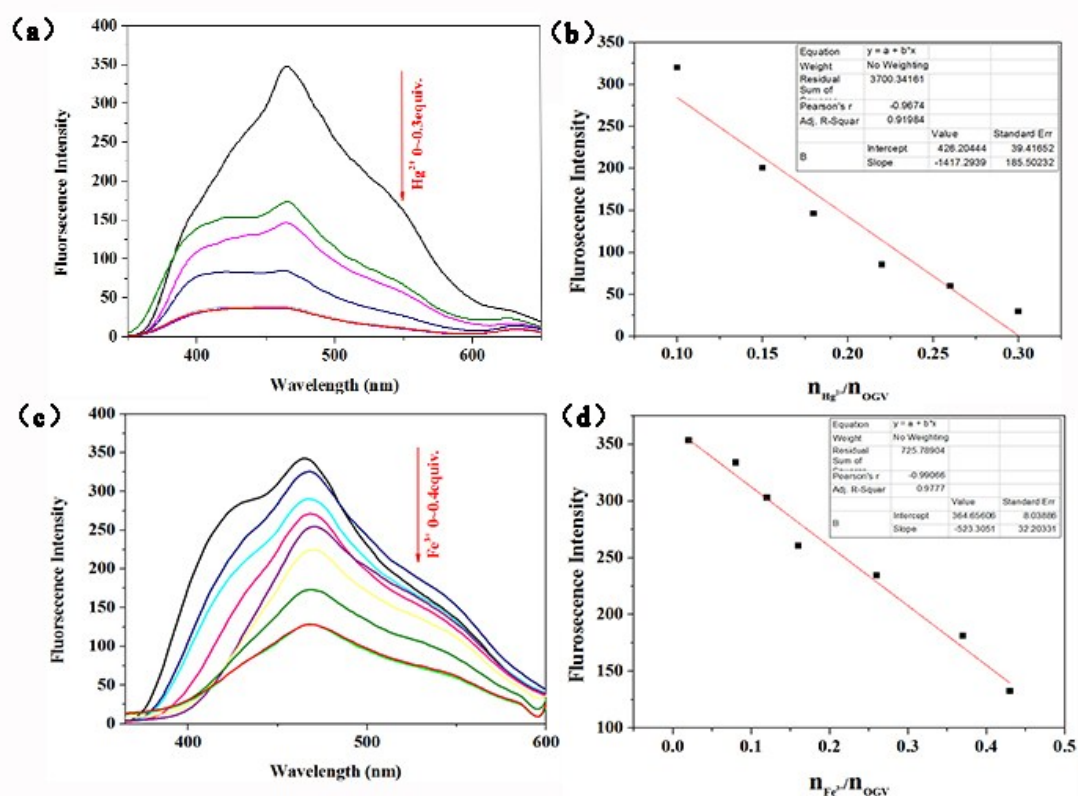


Fig. S6 Fluorescent titration spectra of (a) HgG and (c) FeG and linear fitting of titration curves for (b) HgG and (d) FeG.

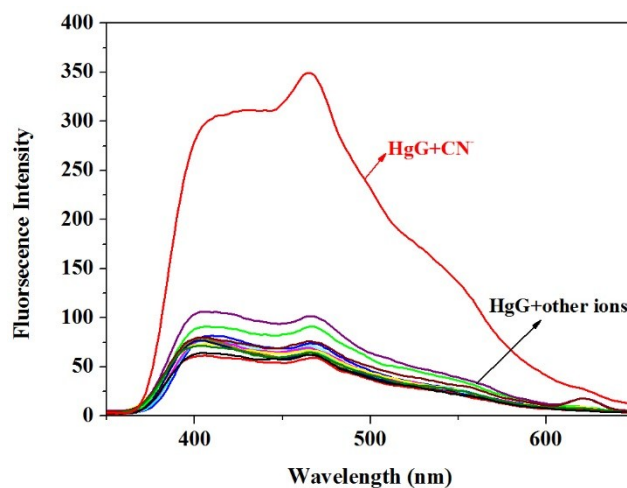


Fig. S7 Fluorescence spectra of HgG (1.0%, in DMSO) in the presence of various anions (F^- ,

Cl^- , Br^- , I^- , AcO^- , H_2PO_4^- , HSO_4^- , N_3^- , SCN^- , S_2^- , ClO_4^- , and CN^-), respectively, using their 0.1 mol L^{-1} sodium or potassium salts water solution as the sources) at room temperature ($\lambda_{\text{ex}}=310 \text{ nm}$).

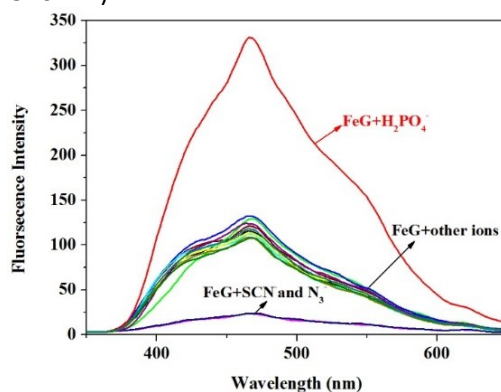


Fig. S8 Fluorescence spectra of FeG (1.0%, in DMSO) in the presence of various anions (F^- , Cl^- , Br^- , I^- , AcO^- , H_2PO_4^- , HSO_4^- , N_3^- , SCN^- , S_2^- , ClO_4^- , and CN^-), respectively, using their 0.1 mol L^{-1} sodium or potassium salts.

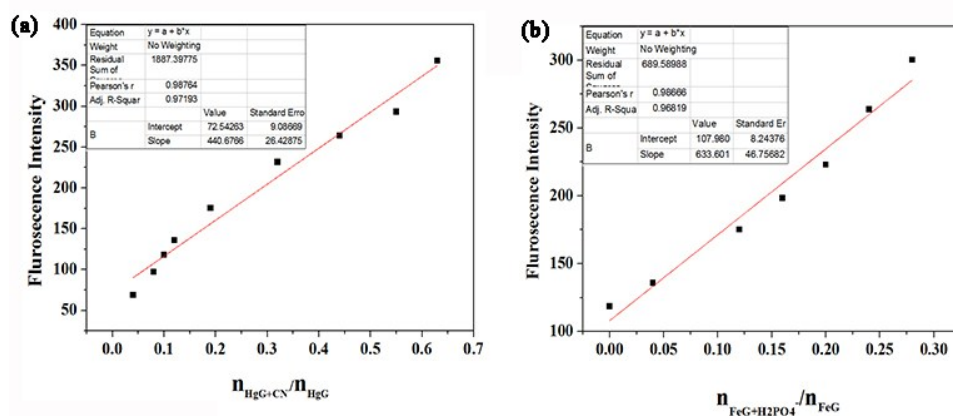


Fig. S9 The linear fitting of titration curves for (a) $\text{HgG}+\text{CN}^-$ and (b) $\text{FeG}+\text{H}_2\text{PO}_4^-$.

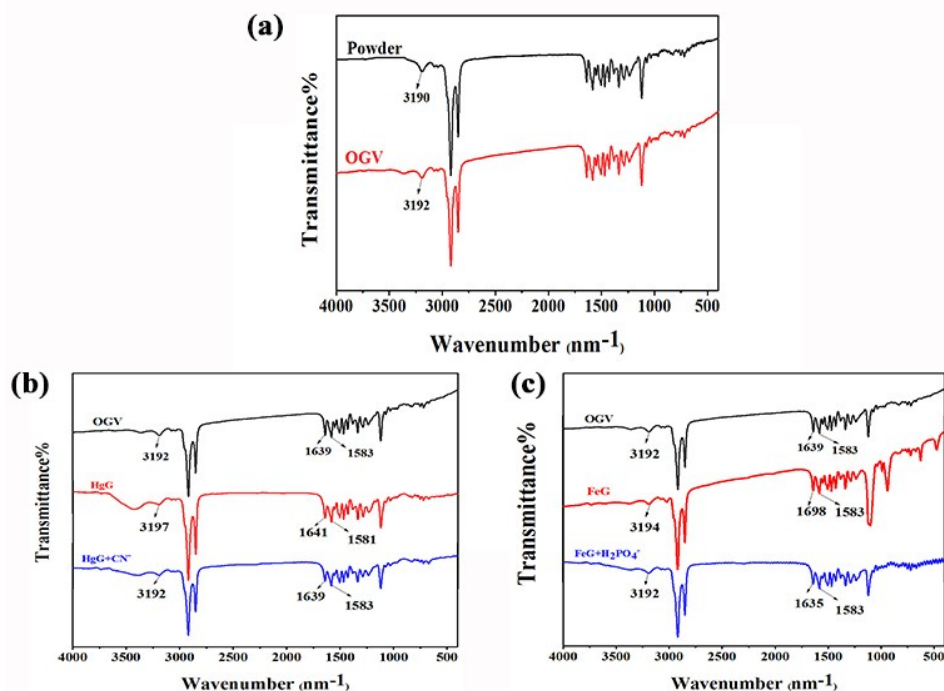


Fig. S10 FT-IR spectra of (a) powder G and xerogel of organogel OGV, (b) xerogel of OGV, HgG and xerogel of HgG treated with CN^- , (c) xerogel of OGV, FeG and xerogel of FeG treated with H_2PO_4^- .

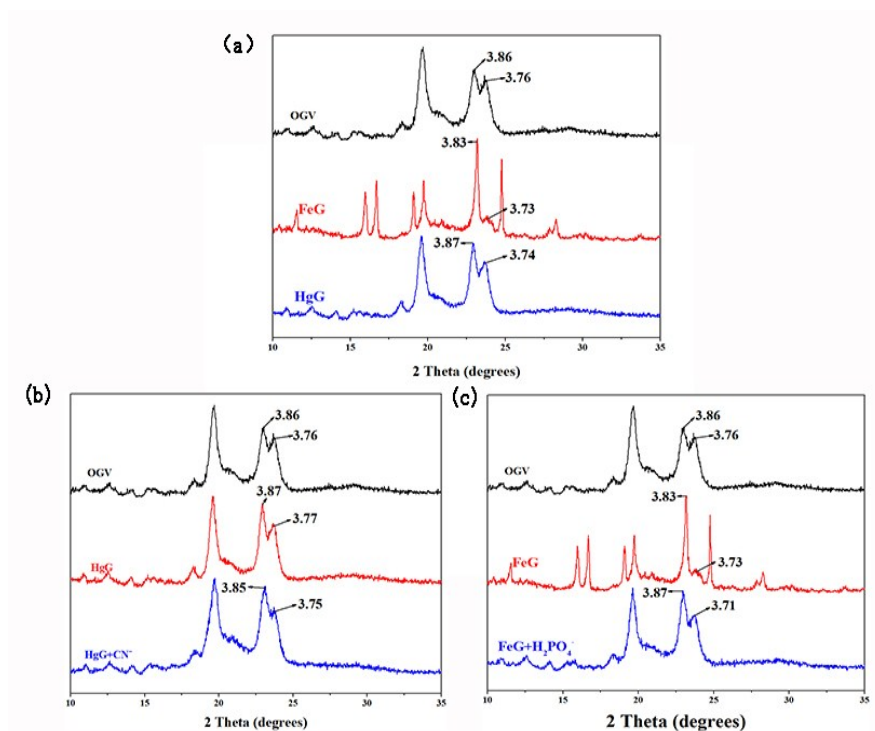


Fig. S11 Powder XRD pattern of (a) organogel OGV and metallogel (HgG and FeG), (b) organogel OGV, HgG and HgG treated with CN^- , (c) organogel OGV, FeG and FeG treated with H_2PO_4^- .

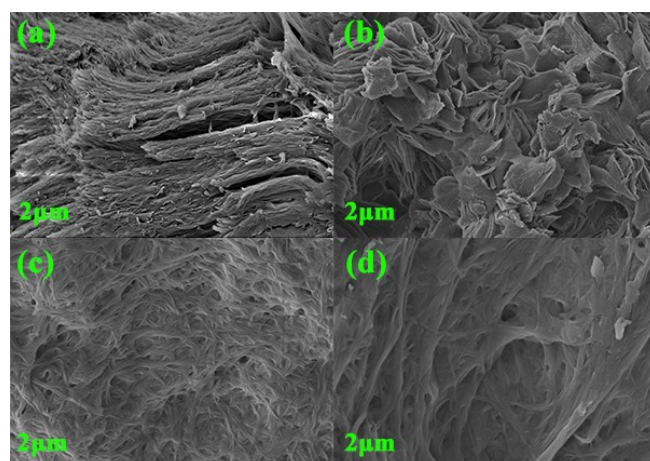


Fig. S12 SEM image of (a) HgG xerogel; (b) FeG xerogel ; (c) HgG xerogel treated with CN^- ; (d) FeG xerogel treated with H_2PO_4^- .